

Article

# A New Strain of *Bacillus tequilensis* CGMCC 17603 Isolated from Biological Soil Crusts: A Promising Sand-Fixation Agent for Desertification Control

Lina Zhao <sup>1,2,3</sup>, Xinrong Li <sup>1,2</sup>, Zengru Wang <sup>1</sup>, Jinghua Qi <sup>1,2,3</sup>, Wenli Zhang <sup>1,2,3</sup>, Yansong Wang <sup>1,2,3</sup> and Yubing Liu <sup>1,2,\*</sup>

<sup>1</sup> Shapotou Desert Research & Experiment Station, Northwest Institute of Eco-Environment and Resources, Chinese Academy of Sciences, Lanzhou 730000, China; zhaolina@lzb.ac.cn (L.Z.); lxinrong@lzb.ac.cn (X.L.); wangzengru@lzb.ac.cn (Z.W.); qijinghua@lzb.ac.cn (J.Q.); zwenli26@126.com (W.Z.); wangyansong18@mailsucas.ac.cn (Y.W.)

<sup>2</sup> Key Laboratory of Stress Physiology and Ecology in Cold and Arid Regions of Gansu Province, Northwest Institute of Eco-Environment and Resources, Chinese Academy of Sciences, Lanzhou 730000, China

<sup>3</sup> University of Chinese Academy of Sciences, Beijing 100049, China

\* Correspondence: liuyb@lzb.ac.cn

Received: 6 October 2019; Accepted: 17 November 2019; Published: 18 November 2019



**Abstract:** In arid and semi-arid desert ecosystems, physical, chemical, and vegetative measures were used to prevent wind erosion. However, studies on the utilization of microbial resources for sand fixation are still limited. To fill this gap, a new strain of *Bacillus tequilensis* CGMCC 17603 with high productivity of exopolysaccharide (EPS) was isolated from biological soil crusts, and its high-density culture technology and sand-fixing ability were studied. The one-factor-at-a-time approach (OFAT) and Box–Behnken design of CGMCC 17603 showed that the optimum culture conditions were pH 8.5, temperature 31 °C, agitation speed 230 rpm, and inoculation quantity 3%, and the optimum medium was 27.25 g/L glucose, 15.90 g/L yeast extract, and 5.61 g/L MgSO<sub>4</sub>•7H<sub>2</sub>O. High-density culture showed that the biomass and EPS yield of CGMCC 17603 increased from 9.62 × 10<sup>7</sup> to 2.33 × 10<sup>9</sup> CFU/mL, and from 8.01 to 15.61 g/L, respectively. The field experiments showed that CGMCC 17603 could effectively improve the ability of sand fixation and wind prevention. These results indicated that *B. tequilensis*, first isolated from cyanobacterial crusts, can be considered as an ideal soil-fixing agent to combat desertification in arid and semi-arid areas.

**Keywords:** *Bacillus tequilensis*; biological soil crusts; Box–Behnken design; desertification control; exopolysaccharide; sand fixation

## 1. Introduction

Desertification is a serious global environmental and ecological problem, affecting ~36 million km<sup>2</sup> of the Earth's terrestrial land surface and ~20% of the world's population [1]. As a country deeply suffering from desertification, the total desertified land in China is about 2.61 million km<sup>2</sup> [2]. Importantly, the desertification mainly caused by wind erosion accounts for more than 70% (about 1.83 million km<sup>2</sup>), affecting millions of people in 13 provinces and causing direct economic losses of about 54.1 billion Yuan/year [2–4].

Mostly, the key to coping with desertification, especially that caused by wind erosion, is to maintain the topsoil stability of sand areas [5]. Biological soil crusts (BSCs) are assemblages of macroscopic (such as cyanobacteria, lichens, and mosses) and microscopic organisms (such as bacteria, fungi, and archaea) that combine with fine soil particles, which have made a positive contribution to the reversion of wind-induced sand erosion [5–8]. Formation of BSCs is a gradually successional process often involving

stages that vary from cyanobacterial to lichen or moss crusts [6,9]. Cyanobacteria, the pioneer species of BSCs, play a significant role in BSC formation and development due to their special adaptability to extreme desert conditions [10], strong aggregation to sand surface particles [11], and excellent improvement of soil fertility [12]. In recent years, cyanobacterial inoculation technology is widely accepted as one of the feasible methods to artificially accelerate the reversal of desertification [5,12–14].

However, metagenomics studies have found that *Bacillus* in bacterial communities also have an irreplaceable position in the early successional stages of BSC succession [15,16]. *Bacillus* is Gram-positive, spore-forming, and widely distributed bacterium [17]. The spores can survive in adverse environments without any deleterious effects on viability and can be rapidly and completely germinated under favorable conditions [18]. Importantly, *Bacillus* play a particularly significant role in resisting erosion through enhancing soil and sediment cohesion, ensuring moisture provision, preventing biotic and abiotic stresses, and facilitating plant and microorganism growth by producing exopolysaccharides (EPS) with comparatively elevated viscosity [12,19,20]. *B. subtilis* [21], *B. thermoantarcticus* [22], *B. licheniformis* [20], *B. coagulans*, and *B. firmus* [23] are the most commonly used functional strains in the production of EPSs. Therefore, application of EPS-producing *Bacillus* sp. might be a promising approach to controlling wind-induced sand erosion in arid and semi-arid deserts.

For this study, our goals were to (i) isolate, screen, and select an EPS-producing *Bacillus* sp., (ii) optimize the fermentation conditions and medium composition of the isolate, and (iii) assess the sand-fixation ability of the isolate. The results of this study can provide new insights into the production and application of simple, low cost, and environmentally friendly sand-fixation agents.

## 2. Materials and Methods

### 2.1. Study Area and Sample Collection

This study was conducted in the Shapotou artificial sand-fixing vegetation area of the Tengger Desert (37°32' N, 105°02' E). The natural landscape of this area comprises large, dense, and reticulate dune chains. The annual average temperature was 10 °C, the mean annual wind velocity is 2.9 m/s, and the annual mean precipitation was 186 mm, with most rainfall occurring during May–September of the year of study [24]. The soil is loose, infertile, mobile, and alkaline, and can thus be classified as Eutric Arenosols in the World Reference Base [25]. The predominant plants are xerophytic shrubs including *Artemisia ordosica* Krasch. and *Caragana korshinskii* Kom. The open areas between the perennial shrubs are covered with cyanobacterial crusts, lichen crusts, and moss crusts.

Cyanobacterial crusts were collected in June 29, 2018. All materials were sampled individually using a sterile stainless steel core sampler (3.5 cm inner diameter). In order to eliminate the influence of micro-topography on the selected samples, six cyanobacterial crusts were collected at least 20 m apart from each other. About 10 g of samples were placed inside a sterile plastic reservoir, transported to the laboratory in a cooler packed with ice, and kept at 4 °C for isolation of *Bacillus* strains.

### 2.2. Isolation and Selection of Candidate *Bacillus* Strain

One gram of each sample was dissolved in 9 mL sterile saline solution (0.9% NaCl w/v) and vortexed at maximum speed (Stomacher 400, Seward Medical, London, UK) for 10 min; then, the suspensions were incubated at 80 °C for 30 min to prepare spores [26]. Next, ten-fold serial dilutions of 100 µL of the suspensions were spread on plates containing Luria-Bertani (LB; 10 g/L tryptone, 5 g/L yeast extract, 10 g/L NaCl, pH 7.0) agar to isolate *Bacillus* strains. The inoculated plates were incubated at 28 °C for 48 h and slimy colonies were picked and purified further by streaking on LB agar. Isolates were stored at –80 °C with cryo-preserved stocks until further analysis.

To further select the candidate *Bacillus* strain, isolates were cultured in 250 mL Erlenmeyer flasks containing 30 mL of LB at 28 °C for 48 h in a rotary shaking incubator at 180 rpm, and then their EPSs were extracted by a modified method described by Abdhul et al. [27]. Briefly, cells were removed by centrifugation at 12,000× g for 20 min at 4 °C, and the resultant supernatant was filtered through

the membrane filter (0.22 µm). The EPS was precipitated upon addition of three volumes of cold ethanol (95%) and stood overnight at 4 °C. Subsequently, the resultant precipitate was recovered by centrifugation at 12,000×g for 20 min at 4 °C, washed three times with 75% ethanol, dried at 60 °C, and re-dissolved in sterile distilled water. The total sugar content of the precipitated EPS was determined by the phenol–sulfuric acid method [28], and glucose was used as standard.

### 2.3. Genetic Identification of Candidate *Bacillus* Strain

Genetic identification was performed by 16S rRNA sequencing [29]. The candidate *Bacillus* strain was grown in LB medium at 28 °C for 48 h in a rotary shaking incubator at 180 rpm. Genomic DNA was extracted and the 16S rRNA was amplified by PCR using primers 27F (5'-AGAGTTTGATCCTGGCTCAG-3') and 1492R (5'-GGTTACCTTGTTACGACTT-3'). Purified 16S rRNA fragment (~1.5 kb) was sequenced by Sangon Biotech (Shanghai) Co., Ltd. (Shanghai, China) and similarity analyses with previously published GenBank sequences were performed using BLAST software at NCBI (<http://www.ncbi.nlm.nih.gov/>). Multiple sequence alignment of DNA was carried out using the Clustal W algorithm in the MEGA software version 5.0 [30]. The neighbor-joining (NJ) method was employed to produce the phylogenetic tree with 1000 bootstrap replications to assess nodal support in the tree, and the *B. subtilis* was used as an out-group strain. Sequence data has been achieved in the GenBank database under the accession number MK177522.

### 2.4. Optimization of Culture Conditions and Medium Composition of Candidate *Bacillus* Strain

#### 2.4.1. One-Factor-at-a-Time Approach (OFAT) Optimization

OFAT, which can effectively screen for significant main factors and their levels [31], was used to screen for optimum culture conditions and medium compositions that affect the biomass yield of the candidate *Bacillus* strain. The culture conditions included temperature, pH, agitation speed, and inoculation quantity, and gradient ranges from 22 to 42 °C (in 3 °C increments), 6.0 to 9.5 (in 0.5 unit increments), 90 to 230 rpm (in 20 rpm increments), and 0.5 to 4.0% (in 0.5% increments), respectively. Each of these conditions was altered one by one while other culture conditions were maintained at a constant level (default values: temperature 28 °C, pH 7.0, agitation speed 180 rpm, inoculation quantity 1%) to study their effects on biomass production of the strain. The parameters estimated in each case were the optical densities monitored at 600 nm.

Moreover, the medium compositions included carbon (C) sources (glucose, maltose, sucrose, dextrin, and lactose), nitrogen (N) sources [peptone, yeast extract, soybean meal, urea, and (NH<sub>4</sub>)<sub>2</sub>SO<sub>4</sub>], and inorganic salts (MgSO<sub>4</sub>•7H<sub>2</sub>O, NaCl, KH<sub>2</sub>PO<sub>4</sub>, CaCO<sub>3</sub>, and MnSO<sub>4</sub>). All C and N sources were industrial grade. The concentrations of the C sources, N sources, and inorganic salts were ranges from 5 to 30 g/L (in 5 g/L increments), 5 to 30 g/L (in 5 g/L increments), and 1 to 11 g/L (in 2 g/L increments), respectively. Each of these factors was altered one by one while the other components of LB medium (default values) were maintained at a constant level. The parameters estimated in each case were the biomass (Colony-Forming Unit/mL, CFU/mL) calculated by ten-fold serial dilutions of 100 µL inoculum.

#### 2.4.2. Response Surface Methodology (RSM) Optimization

RSM, an empirical statistical modeling technique, can minimize the number of experiments required to evaluate several independent variables and their interactions [32,33]. The effects of the main C source (A), main N source (B), and main inorganic salt (C) concentrations (g/L) on the biomass of CGMCC 17603 were studied (Table 1). A three-level (−1, 0, and +1), three-variable Box–Behnken design (BBD) of RSM consisting of 12 full factorial design experiments (runs 1–12) and five replicates in the domain center (runs 13–17) was adopted to estimate the variability of the experimental data (Table 2).

The quadratic polynomial equation for generalized predicting of the optimal point was expressed by Equation (1) as follows:

$$Y = b_0 + b_1A + b_2B + b_3C + b_{11}A^2 + b_{22}B^2 + b_{33}C^2 + b_{12}AB + b_{13}AC + b_{23}BC \quad (1)$$

where Y is the predicted value,  $b_0$  is constant coefficient,  $b_1$ ,  $b_2$ , and  $b_3$  are the linear coefficients,  $b_{11}$ ,  $b_{22}$ , and  $b_{33}$  are the quadratic coefficients, and  $b_{12}$ ,  $b_{13}$ , and  $b_{23}$  are the interaction coefficients.

All of the experimental results are the averages of triplicate runs. Design Expert software 8.0.6 (Stat-Ease Inc., Minneapolis, MN, USA) was used for regression and graphical analysis of the experimental data. Analysis of variance (ANOVA) was used to determine the significance of the main and interaction effects of model terms. Furthermore, we analyzed the biomass and EPS yield of the candidate *Bacillus* strain before and after optimization, inoculums were inoculated into LB medium and optimized medium respectively, and cultured for 0–24 h under unoptimized and optimized culture conditions. After specific time intervals (2 h), the cultures were used to determine EPS concentration (g/L) and calculate biomass yield (CFU/mL).

### 2.5. Field Experimental Design

Field experiments were conducted at the Shapotou artificial sand-fixing vegetation area of the Tengger Desert. The nearby mobile sand was collected, passed through a 2 mm sieve, and put into plastic pots (140 mm in diameter and 110 mm in height) so as to ensure that the acreage of the sand surface was about 500 cm<sup>2</sup>. The candidate *Bacillus* strain was cultured using the optimized medium and culture conditions. For the treatment group, 50 mL of culture broth of the strain was evenly sprayed in a pot, which was equivalent to using 0.1 mL/cm<sup>2</sup> culture broth for these tests. For the control group, the same amount of sterile distilled water was applied. Each group contained four plastic pots. Six months later (September 23, 2018–March 25, 2019), the plastic pots were inverted and removed, and the thickness of soil aggregates were measured. Then, the sand aggregates were carefully placed on the top of the inverted plastic pots and observed for one month (March 25, 2019–April 25, 2019; the average wind velocity >5 m/s) in the natural environment.

### 2.6. Statistical Analysis

ANOVA and Tukey's honest significant difference analysis were performed using SPSS 16.0 (SPSS Inc., Chicago, IL, USA) to determine differences in the EPS yield of isolated *Bacillus* strains, as well as the biomass yield of the candidate *Bacillus* strain at different culture conditions, carbon sources, nitrogen sources, and inorganic salts. Figures were generated using Origin 8.0 (Origin Lab Corp., Northampton, MA, USA).

## 3. Results and Discussion

### 3.1. Screening, Isolation, and Selection of Candidate *Bacillus* Strain

Screening, isolation, and selection of the bacteria were carried out in four steps. First, about 34 *Bacillus* strains were isolated from our samples. Second, some *Bacillus* strains were ignored due to phenotype similarity, reducing the number of selected *Bacillus* strains to 17. Third, 10 strains (designated as *Bacillus* sp. B1, B2, B3, B4, B5, B6, B7, B8, B10, and B12), which all exhibited EPS production capacity, were used to select the candidate *Bacillus* strain (Figure 1). Finally, *Bacillus* sp. B6, showing the most significant capacity to produce EPS ( $P < 0.05$ ; Figure 1), was selected as the candidate *Bacillus* strain for subsequent experiments. Furthermore, molecular identification showed that B6 and *B. tequilensis* 52-LR1-2 (GenBank accession number: MF077125.1) formed a clade with a bootstrap value of 99%, and B6 closely related to *B. subtilis* YH10-11, AU021, and ZHA9 (Figure 2). Similarly, Gatson et al. also confirmed *B. tequilensis* closely related to *B. subtilis* [34]. Therefore, B6

was identified as *B. tequilensis*, and has been preserved in the China General Microbiological Culture Collection Center (CGMCC) with a preservation number of CGMCC 17603.

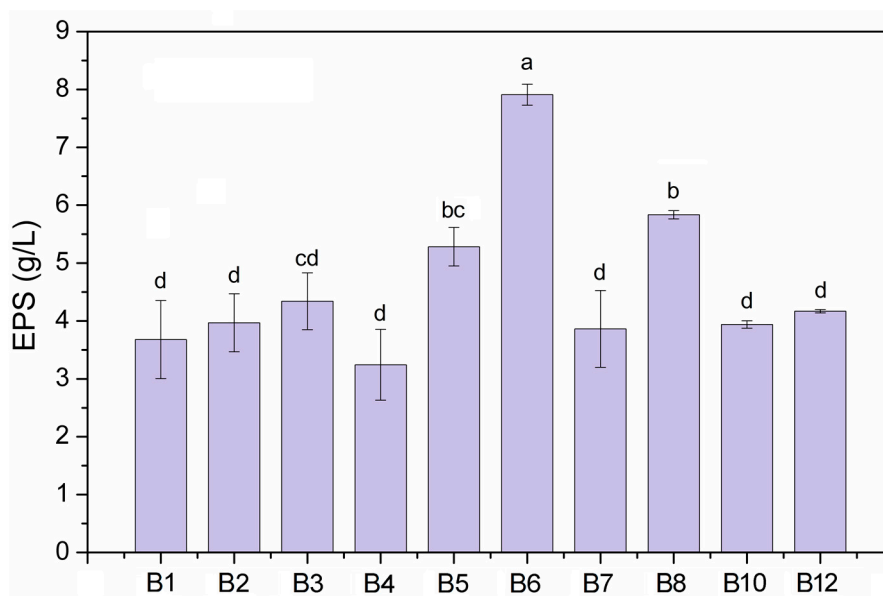


**Figure 1.** Exopolysaccharide (EPS) production of isolated *Bacillus* strains. Different letters represent a significant difference between strains ( $P < 0.05$ ).

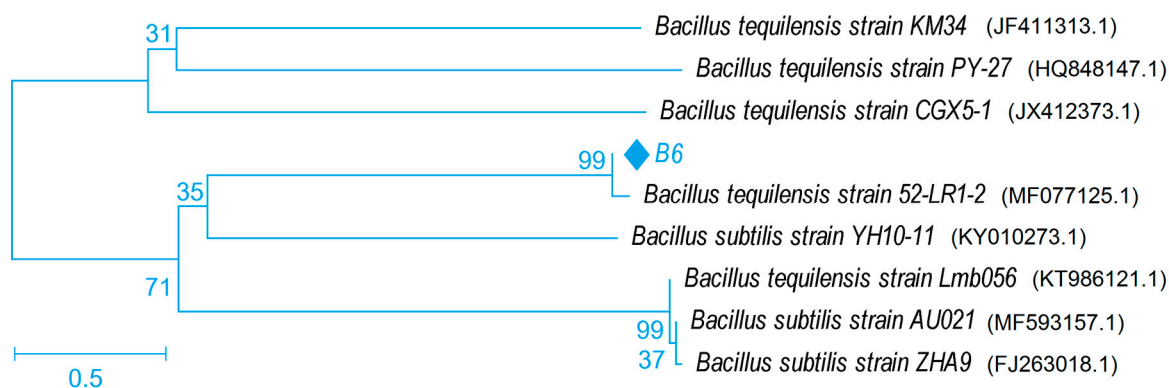


**Figure 2.** Neighbor-joining phylogenetic tree, based on 16S rRNA gene sequences of *Bacillus* sp. B6.

### 3.2. High-Density Culture of *B. Tequilensis* CGMCC 17603

High biomass yield and low cost in the production process are the keys to realizing the popularization and application of *B. tequilensis* CGMCC 17603 in the field of sand fixation. Our study optimized the culture conditions and medium compositions of CGMCC 17603, as these two were the most important factors affecting the production of bacterial biomass and metabolites [35–39]. As shown in Figure 3, the biomass of CGMCC 17603 peaked at temperature 31 °C, pH 8.5, agitation speed 230 rpm, and inoculation quantity 3%. Additionally, the optimal C source, N source, and inorganic salt of CGMCC 17603 were 25 g/L glucose, 15 g/L yeast extract, and 5 g/L  $\text{MgSO}_4 \cdot 7\text{H}_2\text{O}$ , respectively (Figure 4). The results revealed that the OFAT optimization could effectively screen out the optimal levels of key factors, and further confirmed the rationality of factor gradients and the validity of these results [31]. Importantly, industrial-grade glucose and yeast extract are inexpensive and meet our low-cost requirements for culture medium.

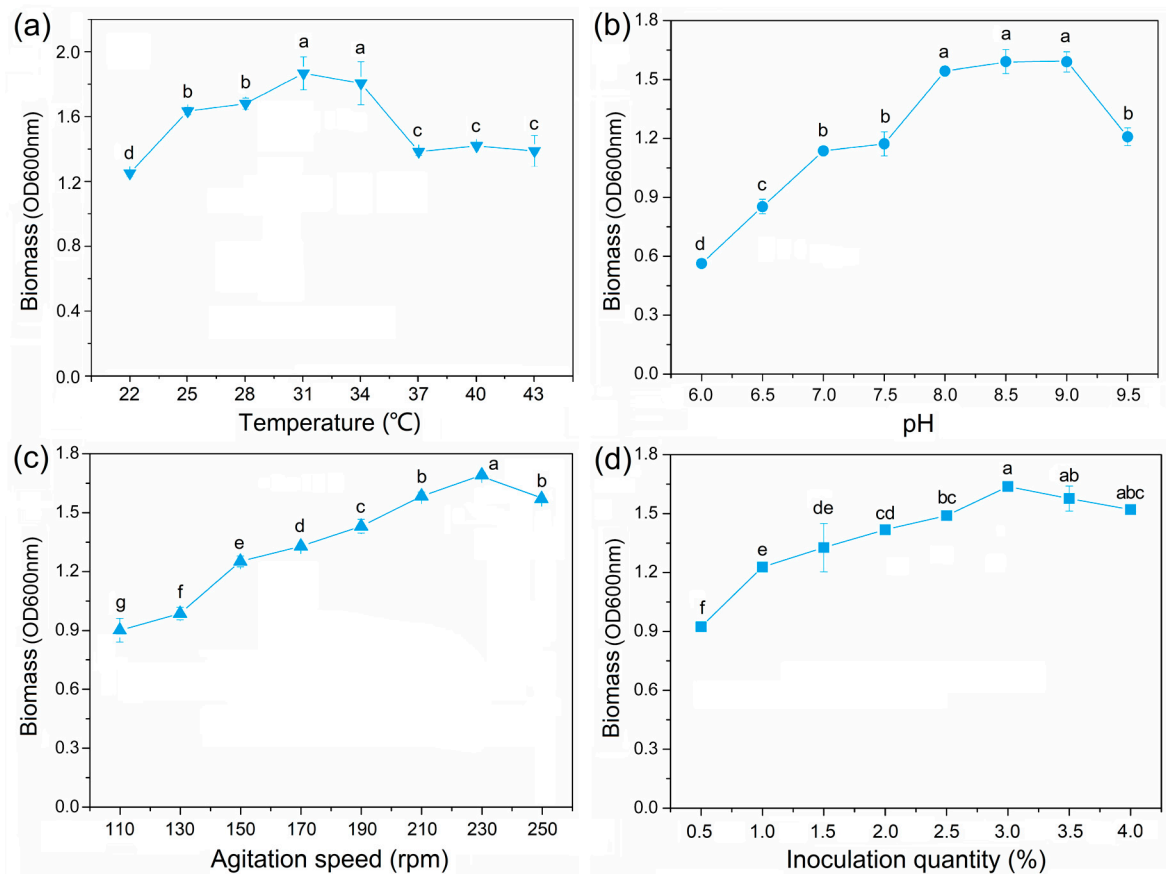


**Figure 3.** Effects of different gradients of temperature (a), pH (b), agitation speed (c), and inoculation quantity (d) on the biomass yield of *B. tequilensis* CGMCC 17603. Different letters represent a significant difference between variables ( $P < 0.05$ ).

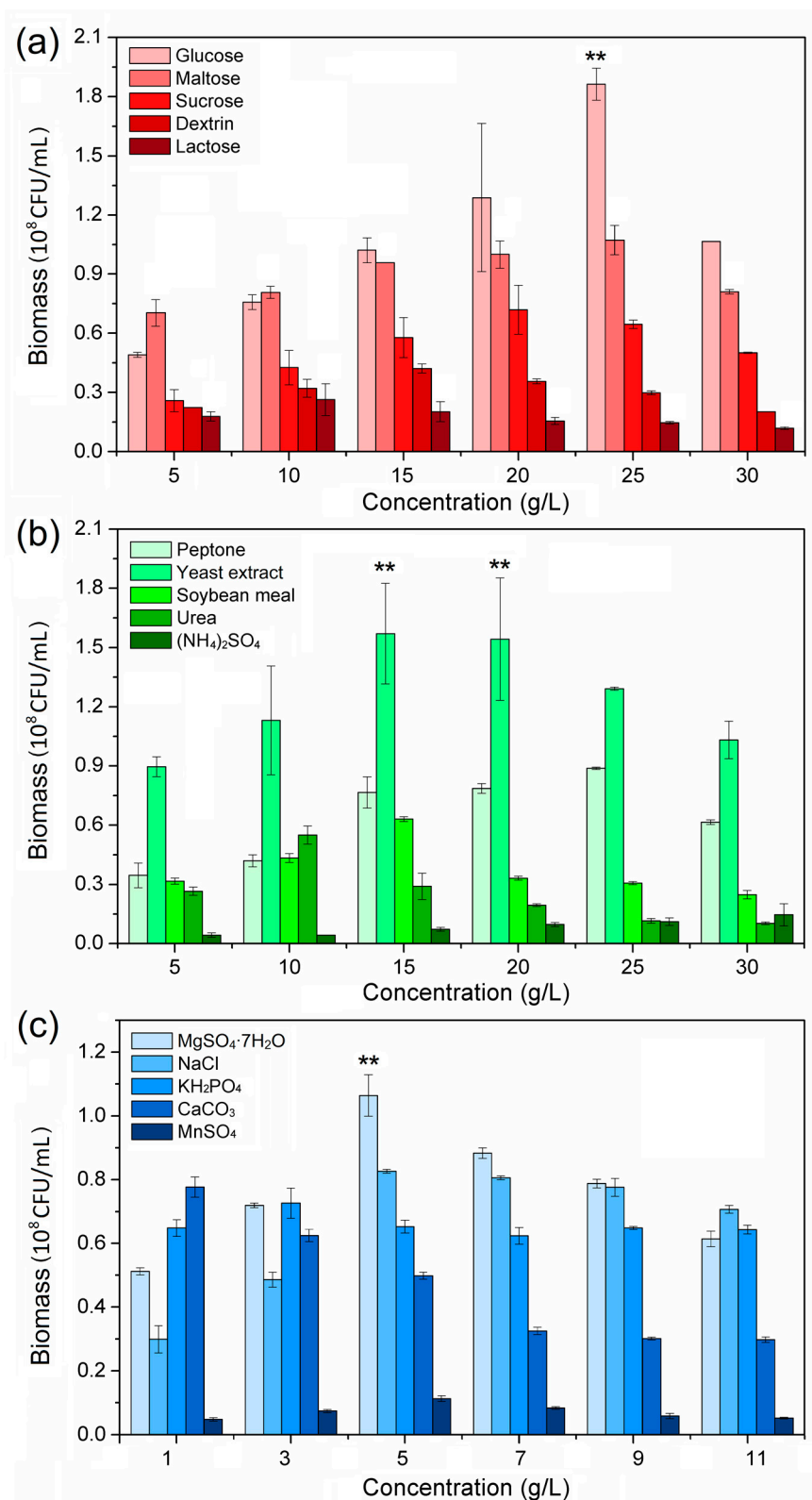


**Figure 4.** Effects of different concentrations of the carbon source (a), nitrogen source (b), and inorganic salt (c) on the biomass yield of *B. tequilensis* CGMCC 17603. \*\* represent a significant difference between variables ( $P < 0.01$ ).

In order to obtain the maximum biomass production and corresponding levels of glucose, yeast extract, and MgSO<sub>4</sub>·7H<sub>2</sub>O (Table 1), 17 experiments with different combinations were designed; their

responses are given in Table 2. The run-17 showed the highest biomass yield up to  $2.340 \times 10^9$  CFU/mL when the medium compositions were set to 25 g/L glucose, 15 g/L yeast extract, and 5 g/L  $\text{MgSO}_4 \cdot 7\text{H}_2\text{O}$  (Table 2). However, when the medium was conducted in compositions of 30 g/L glucose, 10 g/L yeast extract, and 5 g/L  $\text{MgSO}_4 \cdot 7\text{H}_2\text{O}$ , the lowest biomass yield ( $1.875 \times 10^9$  CFU/mL) was attained (Table 2). By applying multiple regression analysis on the actual responses, the Equation (2) was obtained to explain the biomass production:

$$Y = -3.38611 + 0.32213A + 0.1699B + 0.21819C - 1.90 \times 10^{-4}AB + 1.33 \times 10^{-3}AC - 1.75 \times 10^{-4}BC - 6.95 \times 10^{-3}A^2 - 5.15 \times 10^{-3}B^2 - 0.022431C^2 \quad (2)$$

**Table 1.** Independent variables and levels used for Box–Behnken Designs (BBD).

Independent Variables	Symbol Coded	Levels		
		−1	0	+1
Glucose	A	20	25	30
Yeast extract	B	10	15	20
$\text{MgSO}_4 \cdot 7\text{H}_2\text{O}$	C	3	5	7

**Table 2.** BBD matrix for the three independent variables (A: Glucose; B: Yeast extract; C:  $\text{MgSO}_4 \cdot 7\text{H}_2\text{O}$ ) and their corresponding experimental observed responses.

Run	A	B	C	Biomass ( $\times 10^9$ CFU/mL)
1	20	10	5	2.080
2	30	10	5	1.875
3	20	20	5	2.180
4	30	20	5	1.956
5	20	15	3	2.140
6	30	15	3	1.897
7	20	15	7	2.200
8	30	15	7	2.010
9	25	10	3	1.998
10	25	20	3	2.107
11	25	10	7	2.110
12	25	20	7	2.212
13	25	15	5	2.326
14	25	15	5	2.314
15	25	15	5	2.323
16	25	15	5	2.323
17	25	15	5	2.340

When the RSM for yield optimization is applied, the fitness of the model must be verified and guaranteed [40]. Based on the results of ANOVA (Table 3), the coefficient of determination ( $R^2$ ) was 0.9982, indicating that the quadratic model can explain 99.82% of the variability, and merely less than 0.2% of the total variance might occur due to noise that cannot be explained by the model itself [41]. The adjusted  $R^2$  (0.9958; Table 3) also supported a high correlation between the predicted and experimental values. In addition, the model  $F$  value of 423.50,  $P < 0.05$ , and insignificant lack of fit ( $P = 0.3797$ ) implied that all experimental data were adequate as well as the good predictability of the model (Table 3) [42].

The factors of  $A$ ,  $B$ ,  $C$ ,  $AC$ ,  $A^2$ ,  $B^2$ , and  $C^2$  were significant ( $P < 0.05$ ) for biomass production, while other factors demonstrated an insignificant effect ( $P > 0.05$ ; Table 3). The results revealed that the biomass yield of CGMCC 17603 was mainly determined by the linear and quadratic terms of  $A$ ,  $B$ ,  $C$ ,  $AC$ ,  $A^2$ ,  $B^2$ , and  $C^2$  of the model. As  $AC$  (glucose  $\times$   $\text{MgSO}_4 \cdot 7\text{H}_2\text{O}$ ) was statistically significant ( $P = 0.034$ ; Table 3) for biomass production, the optimal levels of glucose and  $\text{MgSO}_4 \cdot 7\text{H}_2\text{O}$  and

the interaction effect on biomass yield were further studied by plotting three-dimensional response surfaces (Figure 5a) and a contour line plot (Figure 5b) when *B* (yeast extract) was kept constant at the level of zero (15 g/L). As shown in Figure 5, glucose closely related to  $\text{MgSO}_4 \cdot 7\text{H}_2\text{O}$ ; more biomass yield was obtained when the concentrations of glucose and  $\text{MgSO}_4 \cdot 7\text{H}_2\text{O}$  were raised from low (−1) to mid-point (0), while further increase would lead to the decrease of the biomass yield.

**Table 3.** Analysis of variance (ANOVA) analysis and statistical parameters of the fitted quadratic polynomial model for the optimization of medium compositions. *A*: Glucose; *B*: Yeast extract; *C*:  $\text{MgSO}_4 \cdot 7\text{H}_2\text{O}$ ; \*: Significant ( $P < 0.05$ ); \*\*: Very significant ( $P < 0.01$ ); ns: Not significant ( $P > 0.05$ ).

Source	Sum of Squares	Degrees of Freedom	Mean Square	F Value	P Value	Significance
Model	0.39	9	0.043	423.5	<0.0001	**
<i>A</i>	0.093	1	0.093	914.05	<0.0001	**
<i>B</i>	0.019	1	0.019	189.03	<0.0001	**
<i>C</i>	0.019	1	0.019	187.1	<0.0001	**
<i>AB</i>	$9.03 \times 10^{-5}$	1	$9.03 \times 10^{-5}$	0.89	0.3774	ns
<i>AC</i>	$7.02 \times 10^{-4}$	1	$7.02 \times 10^{-4}$	6.91	0.034	*
<i>BC</i>	$1.23 \times 10^{-5}$	1	$1.23 \times 10^{-5}$	0.12	0.7386	ns
<i>A</i> <sup>2</sup>	0.13	1	0.13	1250.56	<0.0001	**
<i>B</i> <sup>2</sup>	0.07	1	0.07	686.61	<0.0001	**
<i>C</i> <sup>2</sup>	0.034	1	0.034	333.59	<0.0001	**
Residuals	$7.11 \times 10^{-4}$	7	$1.02 \times 10^{-4}$			
Lack of fit	$3.57 \times 10^{-4}$	3	$1.19 \times 10^{-4}$	1.34	0.3797	ns
Pure error	$3.55 \times 10^{-4}$	4	$8.87 \times 10^{-5}$			
Cor total	0.39	16				
$R^2 = 0.9982$						
Adjusted $R^2 = 0.9958$						

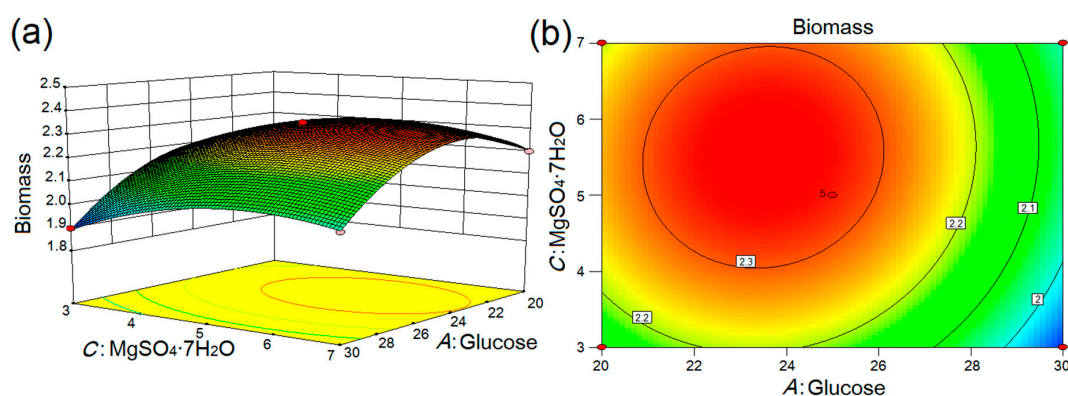


**Figure 5.** The three-dimensional response surface plot (a) and contour line plot (b) of interaction between glucose and  $\text{MgSO}_4 \cdot 7\text{H}_2\text{O}$ .

RSM has provided a set of solutions for predicting the optimum conditions of biomass production of CGMCC 17603. The maximum predicted biomass yield was  $(2.3252 \pm 0.0100) \times 10^9$  CFU/mL when the parameters were set to glucose 27.25 g/L, yeast extract 15.90 g/L, and  $\text{MgSO}_4 \cdot 7\text{H}_2\text{O}$  5.61 g/L. The suitability of the model equation for predicting the optimum response values was tested by using the selected optimal conditions. Under these suggested conditions, the mean value of the biomass yield was  $2.3341 \times 10^9$  CFU/mL and the standard deviation was  $1.2180 \times 10^7$  CFU/mL, which was consistent with the predicted value.

### 3.3. Time Course Studies of *B. tequilensis* CGMCC 17603

The biomass and EPS yields of CGMCC 17603 were monitored over 24 h of fermentation under unoptimized conditions (Figure 6a) and optimized conditions (Figure 6b). In unoptimized conditions, the CGMCC 17603 grew exponentially for the first 8 h of fermentation with no lag phase, reaching a maximum biomass of  $9.62 \times 10^7$  CFU/mL, and then declined slightly during the next 16 h (Figure 6a). Meanwhile, the EPS concentrations increased within the first 12 h to reach a maximum value of 8.01 g/L, and then remained practically constant thereafter (Figure 6a). In the LB medium, CGMCC 17603 performed better than *B. pseudomycoloides* U10 in both the maximum EPS yield and the consumed time [43], suggesting that CGMCC 17603 is a considerable strain under unoptimized conditions. However, the biomass and EPS yield of CGMCC 17603 may be limited by the nutrient elements and proportioning scheme in LB medium and culture conditions.

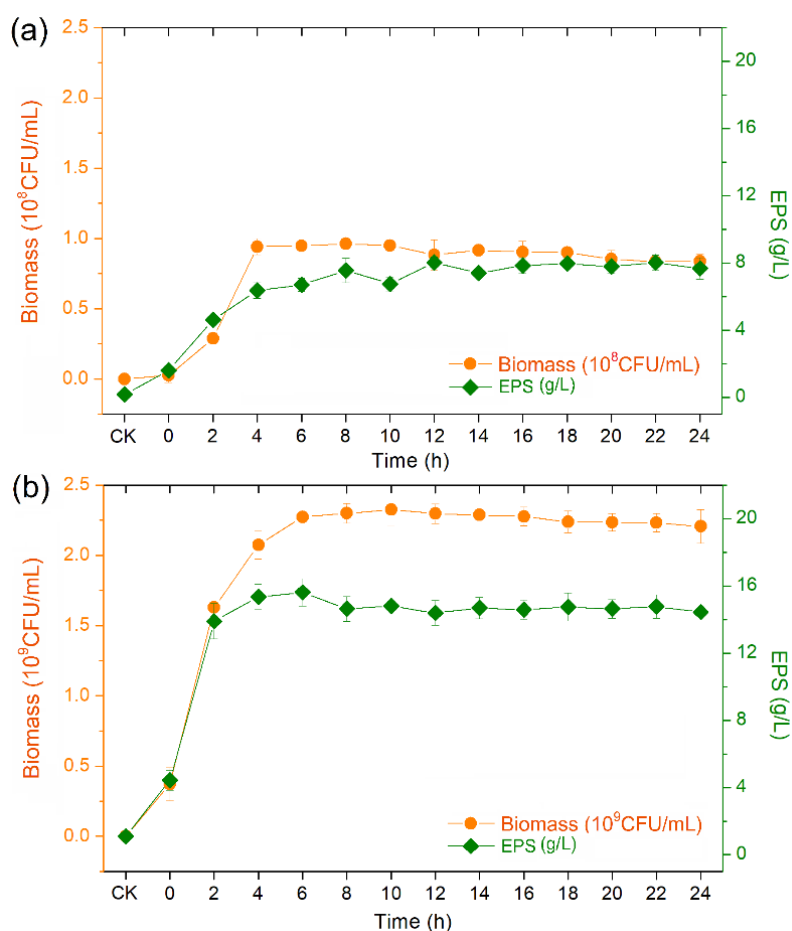


**Figure 6.** Time-course process of fermentation in a 250 mL shake flask for biomass and EPS production by *B. tequilensis* CGMCC 17603 under unoptimized conditions (a) and optimized conditions (b) The unoptimized conditions contained the LB medium, pH 7.0, temperature 28 °C, agitation speed 180 rpm, and inoculation quantity 1%. The optimized conditions contained the optimum medium (27.25 g/L glucose, 15.90 g/L yeast extract, and 5.61 g/L MgSO<sub>4</sub>•7H<sub>2</sub>O), pH 8.5, temperature 31 °C, agitation speed 230 rpm, and inoculation quantity 3%.

In optimized conditions, the exponential growth phase of the CGMCC 17603 lasted for 10 h of fermentation and reached a biomass of  $2.33 \times 10^9$  CFU/mL, which remained practically constant thereafter (Figure 6b). A parallel increase between the EPS concentrations and the biomass was observed during the first 6 h of fermentation, reaching a maximum EPS yield of 15.61 g/L, then declined between 6 h and 12 h, and remained constant afterwards (Figure 6b). The time to obtain the maximum

EPS was much shorter than those of *B. tequilensis* PS21 in a previous study [35], and the EPS yield of CGMCC 17603 (15.61 g/L) was more than that of *B. tequilensis* PS21, *B. tequilensis* FR9 (6.83 g/L), and *B. sonorensis* MJM60315 (8.4 g/L) [35,44,45], indicating that the production mode of CGMCC 17603 can greatly shorten the production time and increase the production efficiency in commercial production. Therefore, we have realized high-density culture of *B. tequilensis* CGMCC 17603 and improvement of EPS yield through low-cost, short-time, and simple production processes, and provided new solutions for the development of strain preparations and EPS preparations.

#### 3.4. Sand-Fixing Property of *B. tequilensis* CGMCC 17603

Before conducting the field experiments, we found that the surface hardness increased within 3 days after spraying the fermented broth of *B. tequilensis* CGMCC 17603 (mainly their EPS), suggesting that EPS of CGMCC 17603 can quickly achieve the first soil stabilization (Appendix A Figure A1). In order to further explore the sand-fixing property of *B. tequilensis* CGMCC 17603, we conducted a six month field experiment in the Shapotou artificial sand-fixing vegetation area of the Tengger Desert. Our study found that after applying the fermentation broth of *B. tequilensis* CGMCC 17603, the sand surfaces of the treatment group closely adhered together with sand and accumulated dusts and sediments (Figure 7a), which is very important for combating wind erosion [5]. However, there was no visible difference between the sand surfaces of the control group and the mobile sand (Figure 7b). These results suggested that the *B. tequilensis* CGMCC 17603 had the potential to promote sand surface stabilization and BSC formation [8]. Moreover, sand of the control group did not aggregate, and the thickness of the aggregate formed by the experimental group was  $5.84 \pm 0.54$  cm (Figure 7c), which proved that the EPS of *B. tequilensis* CGMCC 17603 could fix sand quickly and efficiently. Importantly, there was no significant difference in the thickness of soil aggregates before and after wind erosion ( $5.06 \pm 0.35$  cm,  $P = 0.104$ ; Figure 7d), indicating that soil aggregates formed by the EPS secreted by *B. tequilensis* CGMCC 17603 had good stability and can effectively resist wind erosion.

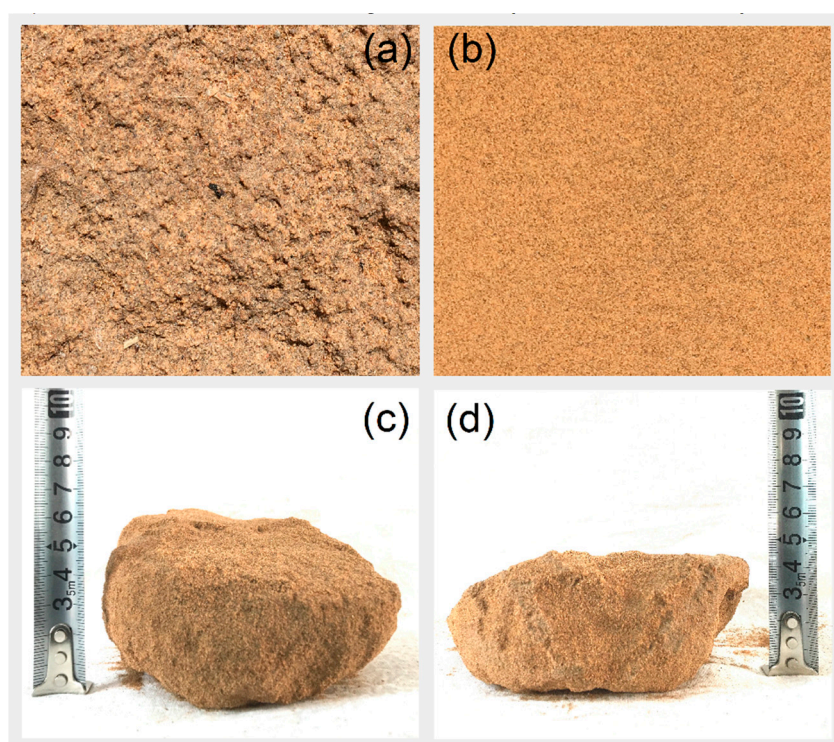


**Figure 7.** Sand-fixing properties of *B. tequilensis* CGMCC 17603. (a) The sand surface of treatment group; (b) the sand surface of control group; (c) the aggregation of sand in treatment group; and (d) the aggregation after one month of natural wind erosion.

#### 4. Conclusions

This study isolated a novel *B. tequilensis* with high EPS yield from the cyanobacterial crusts and further explored its sand-fixing and wind-preventing characteristics in desert ecosystems. Crucially, high-density culture technology significantly improved biomass and EPS yield of *B. tequilensis* CGMCC 17603, laying a good foundation for its popularization and application in the field of sand fixation. Our work confirms the excellent ability of microbial resources as biological sand-fixing agents, and provides a new insight into the efficient, inexpensive, rapid, and environmentally friendly sand-fixing technology serving for relatively arid and semi-arid desert ecosystems. However, long-term monitoring and more in-depth studies of these inoculated *B. tequilensis* CGMCC 17603 are needed to confirm the cost effectiveness of the inoculant and the feasibility for timely combating against desertification, and to explore the mechanisms of soil stabilization by using this strain.

**Author Contributions:** Y.L. and X.L. conceived and designed the experiments. Y.L., L.Z., J.Q., W.Z., and Y.W. performed the experiments. Y.L., L.Z., and Z.W. analyzed the data and prepared figures and tables. Y.L., X.L., and L.Z. contributed significantly to writing and revising the manuscript. All authors reviewed the paper and agreed on both contents and form of the final version.

**Funding:** This work was supported financially by the Strategic Priority Research Program of Chinese Academy of Sciences (grant no. XDA2003010301) and the National Natural Science Foundation of China (grant nos. 41977204 and 41621001).

**Conflicts of Interest:** The authors declare no conflict of interest.

#### Appendix A

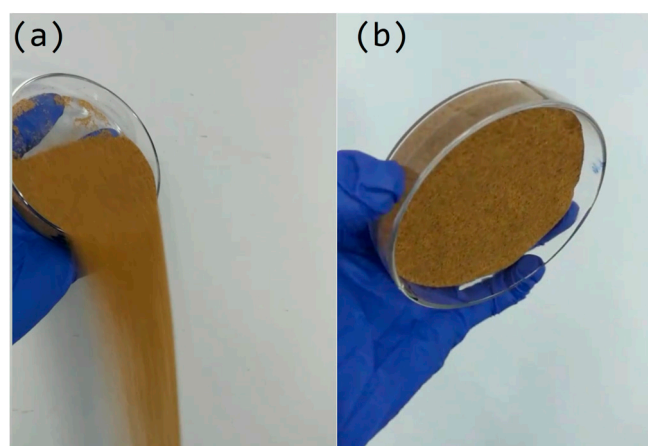


**Figure A1.** Three days after application of 0.1 mL/cm<sup>2</sup> of sterile distilled water (a) and *B. tequilensis* CGMCC 17603 (b).

#### References

1. Middleton, N.J.; Thomas, D.S.G. *World Atlas of Desertification*; Edward Arnold: London, UK, 1992; p. 66.
2. Feng, L.; Jia, Z.; Li, Q. The Dynamic Monitoring of Aeolian Desertification Land Distribution and its Response to Climate Change in Northern China. *Sci. Rep.* **2016**, *6*, 39563. [[CrossRef](#)] [[PubMed](#)]
3. Wang, X.M.; Zhang, C.X.; Hasi, E.; Dong, Z.B. Has the Three Norths Forest Shelterbelt Program solved the desertification and dust storm problems in arid and semiarid China? *J. Arid Environ.* **2010**, *74*, 13–22. [[CrossRef](#)]
4. Xue, Z.; Qin, Z.; Li, H.; Ding, G.; Meng, X. Evaluation of aeolian desertification from 1975 to 2010 and its causes in northwest Shanxi Province, China. *Glob. Planet. Chang.* **2013**, *107*, 102–108. [[CrossRef](#)]
5. Lan, S.; Zhang, Q.; Wu, L.; Liu, Y.; Zhang, D.; Hu, C. Artificially accelerating the reversal of desertification: Cyanobacterial inoculation facilitates the succession of vegetation communities. *Environ. Sci. Technol.* **2013**, *48*, 307–315. [[CrossRef](#)] [[PubMed](#)]

6. Belnap, J.; Weber, B.; Büdel, B. Biological Soil Crusts as an Organizing Principle in Drylands. In *Biological Soil Crusts: An Organizing Principle in Drylands*; Weber, B., Büdel, B., Belnap, J., Eds.; Springer: Cham, Switzerland, 2016; pp. 3–13.
7. Li, X.R.; Xiao, H.L.; Zhang, J.G.; Wang, X.P. Long-Term Ecosystem Effects of Sand-Binding Vegetation in the Tengger Desert, Northern China. *Restor. Ecol.* **2004**, *12*, 376–390. [[CrossRef](#)]
8. Li, X.R.; Zhou, H.Y.; Wang, X.P.; Zhu, Y.G.; O’Conner, P.J. The effects of sand stabilization and revegetation on cryptogam species diversity and soil fertility in the Tengger Desert, Northern China. *Plant. Soil* **2003**, *251*, 237–245. [[CrossRef](#)]
9. Lan, S.; Wu, L.; Zhang, D.; Hu, C. Successional stages of biological soil crusts and their microstructure variability in Shapotou region (China). *Environ. Earth Sci.* **2012**, *65*, 77–88. [[CrossRef](#)]
10. Lan, S.; Wu, L.; Zhang, D.; Hu, C.; Liu, Y.D. Effects of drought and salt stresses on man-made cyanobacterial crusts. *Eur. J. Soil Biol.* **2010**, *46*, 381–386. [[CrossRef](#)]
11. Rossi, F.; Mugnai, G.; Philippis, R.D. Complex role of the polymeric matrix in biological soil crusts. *Plant. Soil* **2018**, *429*, 19–34. [[CrossRef](#)]
12. Acea, M.J.; Prieto-Fernández, A.; Diz-Cid, N. Cyanobacterial inoculation of heated soils: Effect on microorganisms of C and N cycles and on chemical composition in soil surface. *Soil Biol. Biochem.* **2003**, *35*, 513–524. [[CrossRef](#)]
13. Issa, O.M.; Le Bissonnais, Y.; Défarge, C.; Trichet, J. Role of a cyanobacterial cover on structural stability of sandy soils in the Sahelian part of western Niger. *Geoderma* **2001**, *101*, 15–30. [[CrossRef](#)]
14. Jia, R.L.; Li, X.R.; Liu, L.C.; Gao, Y.H.; Zhang, X.T. Differential wind tolerance of soil crust mosses explains their micro-distribution in nature. *Soil Biol. Biochem.* **2012**, *45*, 31–39. [[CrossRef](#)]
15. Liu, L.; Liu, Y.; Zhang, P.; Song, G.; Hui, R.; Wang, Z.; Wang, J. Development of bacterial communities in biological soil crusts along a revegetation chronosequence in the Tengger Desert, northwest China. *Biogeosciences* **2017**, *14*, 3801–3814. [[CrossRef](#)]
16. Liu, L.; Liu, Y.; Hui, R.; Xie, M. Recovery of microbial community structure of biological soil crusts in successional stages of Shapotou desert revegetation, northwest China. *Soil Biol. Biochem.* **2017**, *107*, 125–128. [[CrossRef](#)]
17. Schallmeyer, M.; Singh, A.; Ward, O.P. Developments in the use of *Bacillus* species for industrial production. *Can. J. Microbiol.* **2004**, *50*, 1–17. [[CrossRef](#)]
18. Nicholson, W.L.; Munakata, N.; Horneck, G.; Melosh, H.J.; Setlow, P. Resistance of *Bacillus* endospores to extreme terrestrial and extraterrestrial environments. *Microbiol. Mol. Biol. Rev.* **2000**, *64*, 548–572. [[CrossRef](#)]
19. Flemming, H.C.; Neu, T.R.; Wozniak, D.J. The EPS matrix: The “house of biofilm cells”. *J. Bacteriol.* **2007**, *189*, 7945–7947. [[CrossRef](#)]
20. Ghaly, A.; Arab, F.; Mahmoud, N.; Higgins, J. Production of levan by *Bacillus licheniformis* for use as a soil sealant in earthen manure storage structures. *Am. J. Biotechnol. Biochem.* **2007**, *3*, 47–54.
21. Razack, S.A.; Velayutham, V.; Thangavelu, V. Influence of various parameters on exopolysaccharide production from *Bacillus subtilis*. *Int. J. ChemTech Res.* **2013**, *5*, 2221–2228.
22. Manca, M.C.; Lama, L.; Improta, R.; Esposito, E.; Gambacorta, A.; Nicolaus, B. Chemical composition of two exopolysaccharides from *Bacillus thermoantarcticus*. *Appl. Environ. Microbiol.* **1996**, *62*, 3265–3269.
23. Szumigaj, J.; Zakowska, Z.; Klimek, L. Exopolysaccharide production by *Bacillus* strains colonizing packaging foils. *Pol. J. Microbiol.* **2008**, *57*, 281–287. [[PubMed](#)]
24. Li, X.R.; Jia, R.L.; Zhang, Z.S.; Zhang, P.; Hui, R. Hydrological response of biological soil crusts to global warming: A ten-year simulative study. *Glob. Chang. Boil.* **2018**, *24*, 4960–4971. [[CrossRef](#)] [[PubMed](#)]
25. FAO. *World Reference Base for Soil Resources*; World Soil Resources Report No. 84; FAO: Rome, Italy, 1998.
26. Feijoo, S.C.; Hayes, W.W.; Watson, C.E.; Martin, J.H. Effects of microfluidizer® technology on *Bacillus licheniformis* spores in ice cream mix. *J. Dairy Sci.* **1997**, *80*, 2184–2187. [[CrossRef](#)]
27. Abdhul, K.; Ganesh, M.; Shanmughapriya, S.; Kanagavel, M.; Anbarasu, K.; Natarajaseenivasan, K. Antioxidant activity of exopolysaccharide from probiotic strain *Enterococcus faecium* (BDU7) from Ngari. *Int. J. Boil. Macromol.* **2014**, *70*, 450–454. [[CrossRef](#)]
28. Dubois, M.; Gilles, K.A.; Hamilton, J.K.; Rebers, P.A.; Smith, F. Colorimetric method for determination of sugars and related substances. *Anal. Chem.* **1956**, *28*, 350–356. [[CrossRef](#)]
29. Sambrook, J.; Fritsch, E.F.; Maniatis, T. *Molecular Cloning: A Laboratory Manual*; Cold Spring Harbor Laboratory Press: Woodbury, NY, USA, 1989.

30. Tamura, K.; Peterson, D.; Peterson, N.; Stecher, G.; Nei, M.; Kumar, S. MEGA5: Molecular evolutionary genetics analysis using maximum likelihood, evolutionary distance, and maximum parsimony methods. *Mol. Biol. Evol.* **2011**, *28*, 2731–2739. [[CrossRef](#)] [[PubMed](#)]
31. Mcdaniel, W.R.; Ankenman, B.E. Comparing experimental design strategies for quality improvement with minimal changes to factor levels. *Qual. Reliab. Eng. Int.* **2000**, *16*, 355–362. [[CrossRef](#)]
32. Ravikumar, K.; Krishnan, S.; Ramalingam, S.; Balu, K. Optimization of process variables by the application of response surface methodology for dye removal using a novel adsorbent. *Dye. Pigment.* **2007**, *72*, 66–74. [[CrossRef](#)]
33. Amenaghawon, N.A.; Nwaru, K.I.; Aisien, F.A.; Ogbeide, S.E.; Okieimen, C.O. Application of Box-Behnken design for the optimization of citric acid production from corn starch using *Aspergillus niger*. *Biotechnol. J. Int.* **2013**, 236–245. [[CrossRef](#)]
34. Gatson, J.W.; Benz, B.F.; Chandrasekaran, C.; Satomi, M.; Venkateswaran, K.; Hart, M.E. *Bacillus tequilensis* sp. nov., isolated from a 2000-year-old Mexican shaft-tomb, is closely related to *Bacillus subtilis*. *Int. J. Syst. Evol. Microbiol.* **2006**, *56*, 1475–1484. [[CrossRef](#)]
35. Luang-In, V.; Saengha, W.; Deeseenthum, S. Characterization and bioactivities of a novel exopolysaccharide produced from lactose by *Bacillus tequilensis* PS21 isolated from Thai Milk Kefir. *Microbiol. Biotechnol. Lett.* **2018**, *46*, 9–17. [[CrossRef](#)]
36. Rao, Y.K.; Tsay, K.J.; Wu, W.S.; Tzeng, Y.M. Medium optimization of carbon and nitrogen sources for the production of spores from *Bacillus amyloliquefaciens* B128 using response surface methodology. *Process. Biochem.* **2007**, *42*, 535–541. [[CrossRef](#)]
37. Kumar, V.; Sahai, V.; Bisaria, V. High-density spore production of *Piriformospora indica*, a plant growth-promoting endophyte, by optimization of nutritional and cultural parameters. *Bioresour. Technol.* **2011**, *102*, 3169–3175. [[CrossRef](#)] [[PubMed](#)]
38. Luang-In, V.; Deeseenthum, S. Exopolysaccharide-producing isolates from Thai milk kefir and their antioxidant activities. *Lwt-Food Sci. Technol.* **2016**, *73*, 592–601. [[CrossRef](#)]
39. Freitas, F.; Alves, V.D.; Pais, J.; Carvalheira, M.; Costa, N.; Oliveira, R.; Reis, M.A. Production of a new exopolysaccharide (EPS) by *Pseudomonas oleovorans* NRRL B-14682 grown on glycerol. *Process. Biochem.* **2010**, *45*, 297–305. [[CrossRef](#)]
40. ElMekawy, A.; F El-Baz, A.; A Soliman, E.; Hudson, S. Statistical modeling and optimization of chitosan production from *Absidia coerulea* using response surface methodology. *Curr. Biotechnol.* **2013**, *2*, 125–133. [[CrossRef](#)]
41. Wee, L.L.; Annuar, M.S.M.; Ibrahim, S.; Chisti, Y. Enzyme-mediated production of sugars from sago starch: Statistical process optimization. *Chem. Eng. Commun.* **2011**, *198*, 1339–1353. [[CrossRef](#)]
42. Amouzgar, P.; Khalil, H.A.; Salamatinia, B.; Abdullah, A.Z.; Issam, A.M. Optimization of bioresource material from oil palm trunk core drying using microwave radiation; a response surface methodology application. *Bioresour. Technol.* **2010**, *101*, 8396–8401. [[CrossRef](#)]
43. Solmaz, K.; Ozcan, Y.; Mercan Dogan, N.; Bozkaya, O.; Ide, S. Characterization and Production of Extracellular Polysaccharides (EPS) by *Bacillus Pseudomycooides* U10. *Environments* **2018**, *5*, 63. [[CrossRef](#)]
44. Rani, R.P.; Anandharaj, M.; Sabhathathy, P.; Ravindran, A.D. Physicochemical and biological characterization of novel exopolysaccharide produced by *Bacillus tequilensis* FR9 isolated from chicken. *Int. J. Boil. Macromol.* **2016**, *96*, 1–10. [[CrossRef](#)]
45. Palaniyandi, S.A.; Damodharan, K.; Suh, J.W.; Yang, S.H. Functional characterization of an exopolysaccharide produced by *Bacillus sonorensis* MJM60135 isolated from Ganjang. *J. Microbiol. Biotechnol.* **2018**, *28*, 663–670. [[CrossRef](#)] [[PubMed](#)]

